Commissioning of the camera of the first Large Size Telescope of the Cherenkov Telescope Array

T. Saito,[a,*] C. Delgado,[b] O. Blanch,[c] M. Artero,[c] J. A. Barrio,[d] F. Cassol,[e] C. Diaz,[b] D. Hadasch,[a] D. Hoffmann,[e] J. Houles,[e] Y. Inome,[a] M. Iori,[f] L. Jouvin,[c] D. Kerszberg,[c] Y. Kobayashi,[a] H. Kubo,[g] G. Martinez,[b] D. Mazin,[a] E. Moretti,[c] T. Nakamori,[h] S. Nozaki,[g] T. Oka,[g] A. Okumura,[i] M. Palatiello,[f] M. Polo,[b] J. Prast,[k] S. Sakurai,[a] Y. Sunada,[j] M. Takahashi,[a] R. Takeishi,[a] L. A. Tejedor,[d] T. Yamamoto[l] and T. Yoshida[m] for the CTA LST project

(a complete list of authors can be found at the end of the proceedings)

a) ICRR, University of Tokyo, 5-1-5, Kashiwa-no-ha, Kashiwa, Chiba 277-8582, Japan; b) CIEMAT, Avda. Complutense 40, 28040 Madrid, Spain: c) Institut de Fisica d'Altes Energies (IFAE), The Barcelona Institute of Science and Technology, Campus UAB, 08193 Bellaterra (Barcelona), Spain; d) EMFTEL department and IPARCOS, Universidad Complutense de Madrid, 28040 Madrid, Spain; e) Aix-Marseille Université, CNRS/IN2P3, CPPM, 163 Avenue de Luminy, 13288 Marseille cedex 09, France; f) INFN Sezione di Roma La Sapienza, P.le Aldo Moro, 2 - 00185 Roma, Italy; g)Graduate School of Science, Kyoto University, Sakyo-ku, Kyoto, 606-8502, Japan; h) Department of Physics, Yamagata University, Yamagata, Yamagata 990-8560, Japan; i) ISEE, Nagoya University, Chikusa-ku, Nagoya 464-8602, Japan, j) Grad. Sch. of Sci. and Eng., Saitama University, 255 Simo-Ohkubo, Sakura-ku, Saitama 338-8570, Japan; k) CNRS, Laboratoire d'Annecy de Physique des Particules - IN2P3, 74000 Annecy, France; l) Department of Physics, Konan University, Kobe, Hyogo, 658-8501, Japan: m) Faculty of Science, Ibaraki University, Mito, Ibaraki, 310-8512, Japan

ABSTRACT

The first Large Size Telescope (LST-1) of the Cherenkov Telescope Array has been operational since October 2018 at La Palma, Spain. We report on the results obtained during the camera commissioning. The noise level of the readout is determined as a 0.2 p.e. level. The gain of PMTs are well equalized within 2% variation, using the calibration flash system. The effect of NSB on the signal readout noise as well as the PMT gain estimation are also well evaluated. Trigger thresholds are optimized for the lowest possible gamma-ray energy threshold and the trigger distribution synchronization has been achieved within 1 ns precision. Automatic rate control realizes the stable observation with 1.5% rate variation over 3 hours. The performance of the novel DAQ system demonstrates a less than 10% dead time for 15 kHz trigger rate even with sophisticated online data correction.

+++

1. LST camera overview

The camera of LST is shown in Figure 1. It consists of 265 modules, each of which is equipped with 7 PMTs. The digital trigger signal is generated in each module and propagated through backplanes (BPs) to the trigger interface board (TIB) installed at the top left corner of the camera. If conditions are met, the readout trigger is sent from TIB to each modules through BPs. Upon the triggers, the events are readout with the DAQ system.

A movable image screen is also equipped. A star image can be focused on it, which is useful to calibrate the mirror alignment and telescope pointing.

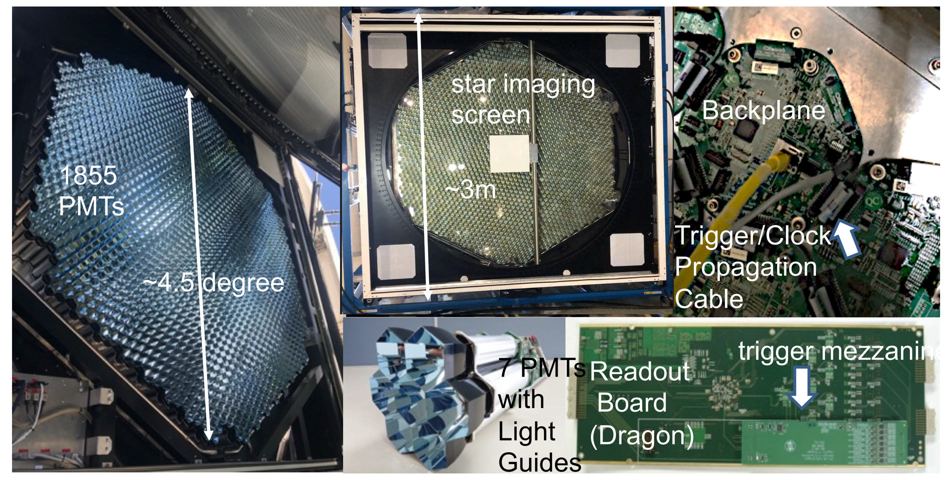

Figure 1: LST Camera (Left). It consists of 265 modules, each of which is equipped with 7 PMTs (bottom center). An analog trigger system (bottom right) is implemented where PMT signals from 3 modules (21 pixels) are summed up before a discriminator. The readout trigger signal is distributed through backplanes (top right).

2. Noise level

Figure 2 (Left) shows the noise level (pedestal standard deviation) as a function of the NSB level. The noise level with the shutter closed and HVs on corresponding to 0.21 p.e.. It gets higher with higher anode currents. A fitting function indicates that the relation is explained by a square root function. Figure 2 (Right) shows the noise level is stable at 1% level (peak to peak) for 3 hours.

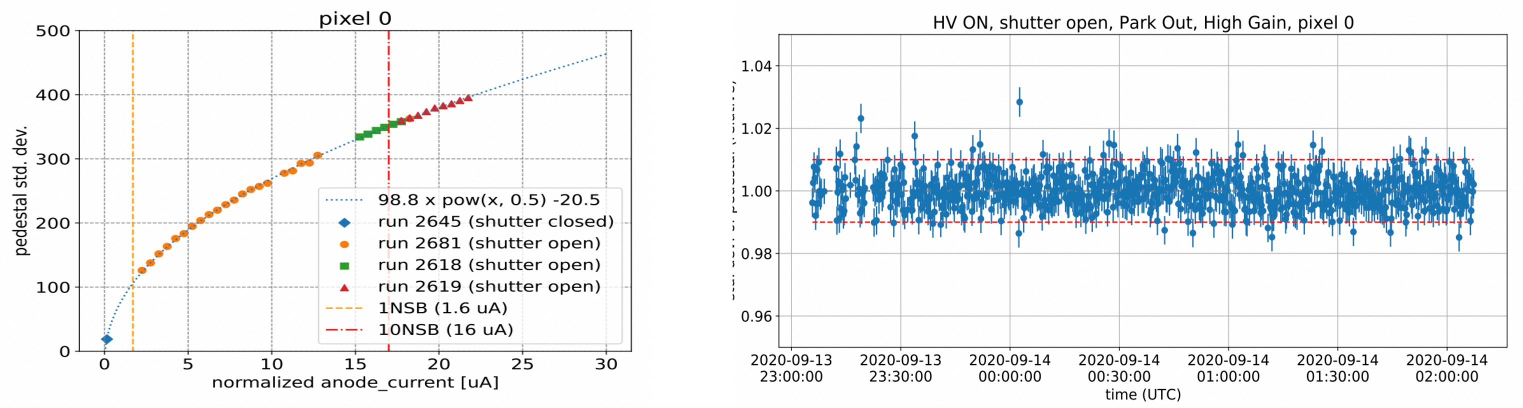

Figure 2: (left) Noise level during multiple observation runs as a function of the anode current. Orange and red dotted lines show dark NSB and 10 times higher than dark NSB level, respectively. (right) Time evolution of the noise for a characteristic single pixel for three hours..

3. PMT gain flat-fielding and calibration

PMT gain flat-fielding and absolute gain calibration are achieved using the Calibration Box. The estimation of absolute calibration coefficients (ADC/p.e) is achieved through the so-called F-Factor method

- After HV adjustment, a charge relative dispersion is less than 2 (3)% and 3% for the high (low) gain (Figure 3.)
- The variation over time for one pixel is ~ 0.5%.
- The calibration results are influenced by the NSB up to less than 2% at 10 x dark NSB (Figure. 4)

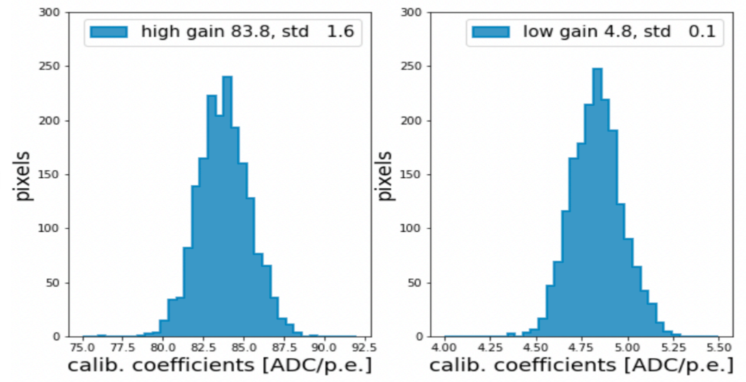

Figure 3: Pixel calibration coefficients estimated with the F-Factor method for high gain (left) and low gain (right) channel.

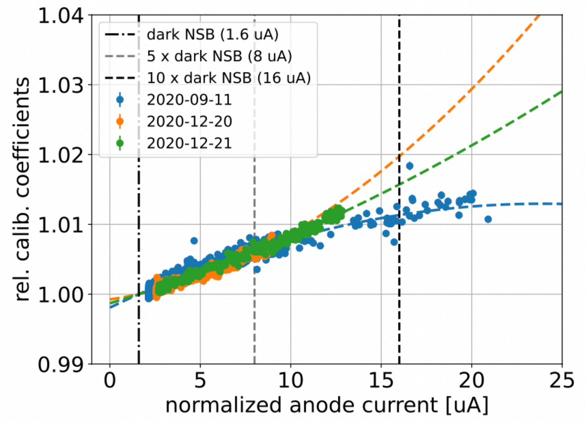

Figure 4: Time evolution of relative calibration coefficients (camera average) as function of the anode current. Vertical lines indicate anode current values which correspond to different NSB levels (dark NSB corresponds to 1.6 μA).

4. Trigger tuning

The trigger system consists of two trigger levels (L0 and L1), the TIB and the BPs.

- L0: Acting at individual pixel level, adjusting the path length and amplitude.
- L1: Signal from a region of 21 neighbour pixels are summed up and examined at the module. A local camera trigger is raised if any of the summed signal is above the threshold (DT)
- BP: Trigger signals from/to the modules are propagated via BPs. Specific delays are defined in each BP so that the timing of the trigger from/to the modules are equalized (See Figure 5).
- TIB: Examine the trigger inputs and busy state of readout, and if appropriate, sends the trigger signal to the modules

L1 threshold values are chosen such that

- It provides maximum rate in all trigger regions
- keeping them all out of the NSB dominated region
- for any NSB conditions (See Figure 6)

The uniformity of the center of gravity of shower images

- 22% below 50 photoelectrons
- 7% at the analysis threshold

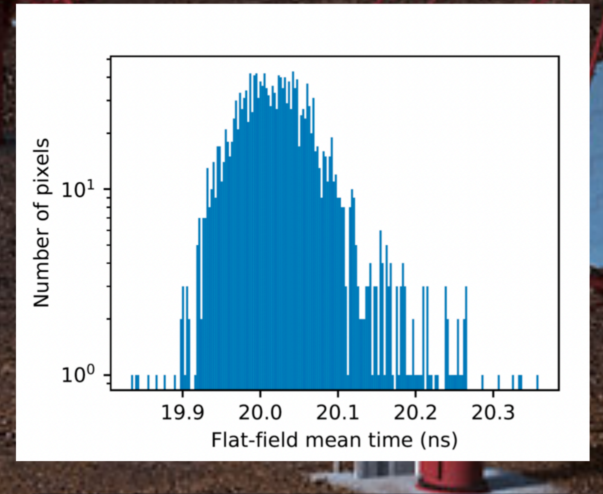

Figure 5: Flatfield mean time distributions of trigger timing for all pixels. The standard deviation of the distribution is 150 ps.

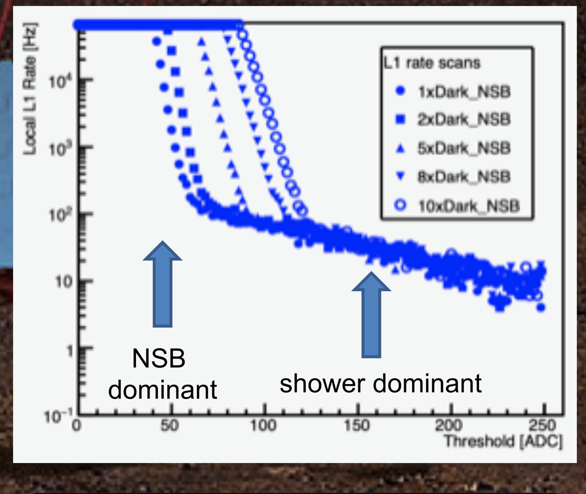

Figure 6: L1 trigger rate at different NSB conditions provided by a characteristic 21 pixel trigger region as a function of the Discriminator Threshold applied.

5. DAQ performance

The network architecture of the DAQ system is schematically explained in Figure 7. The DAQ software in the camera server

- builds a camera event,
- selects one of the two gains
- subtracts readout pedestal

The performance of the DAQ system for the fixed frequency case and the random trigger case are presented in Figure 8.

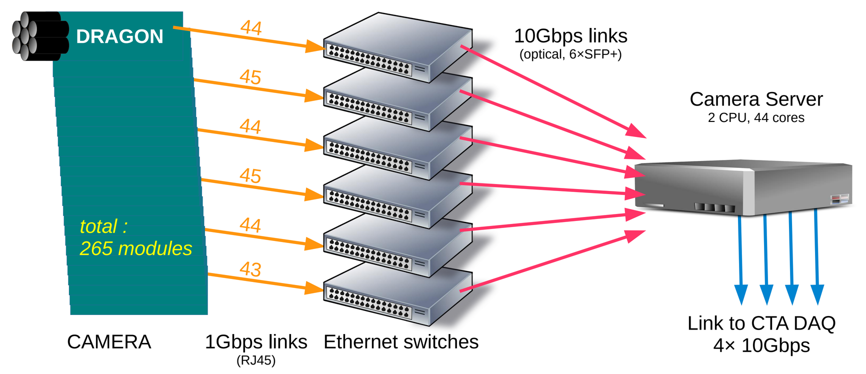

Figure 7 The front-end boards send data through 265 1-Gbps Ethernet links, which are concentrated in six 10-Gbps Ethernet links by a set of six Ethernet switches. These data are received by the camera server equipped with custom tailored software for data assembly and preprocessing.

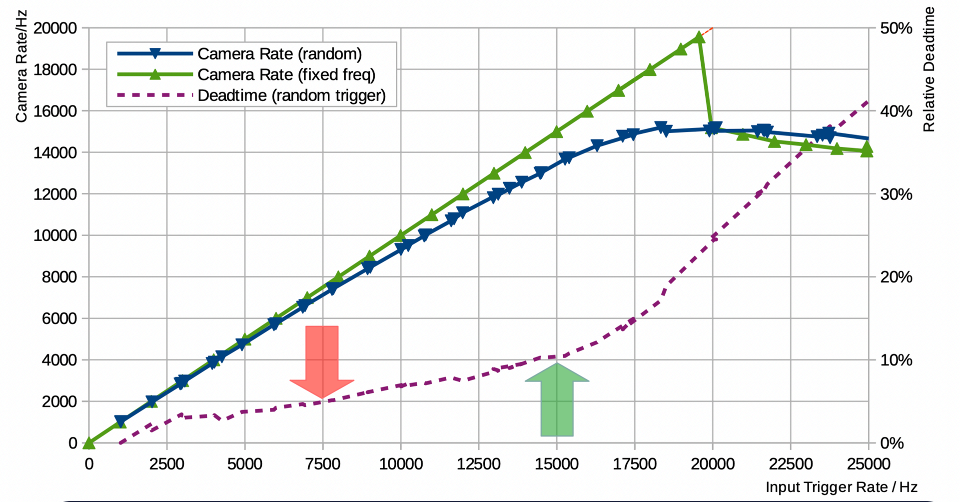

Figure 8: Event output rate for randomly triggered events and triggers with constant delays (frequency) and deadtime (random trigger only) as a function of trigger input: The requirements on deadtime (< 5% at 7 kHz, red arrow) and minimal sustainable rate (15 kHz, green arrow) are fulfilled.

6. Stability of data taking

To achieve stable observations with changing sky conditions, the online rate control is designed to modify the thresholds on the fly.

- Level 0: If the pixel trigger rate is above 10 times the expected pixel rate, then this pixel is excluded from the sum-trigger at each module
- Leve 1: The rate R of a given module is monitored and R_{max}, R_{target}, R_{min} are pre-defined.
  - In case $R > R_{max}$, the threshold is increased until $R < R_{target}$
  - In case $R < R_{min}$, the threshold is decreased until $R > R_{target}$

Figure 9 illustrates an example of the rate control. Figure 10 shows the time evolution of the rates during the standard data. The rate can be described as $R_0 \cos(zenith)^{0.72}$. and stable within a standard deviation of 1.5% during the 3-hours observations.

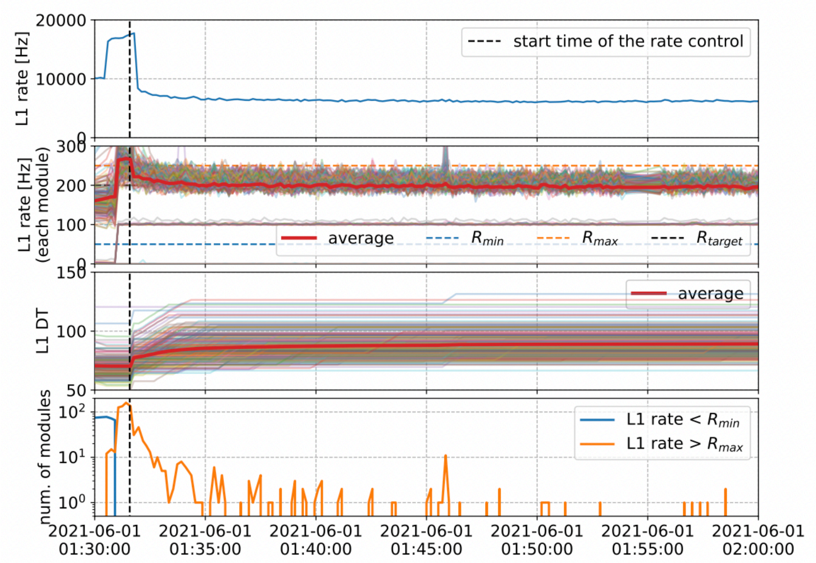

Figure 9 Behaviour of the rate control. From the top, L1 total rate, L1 module rate, L1 DT, and a number of modules affected by the rate control are shown as a function of the time.

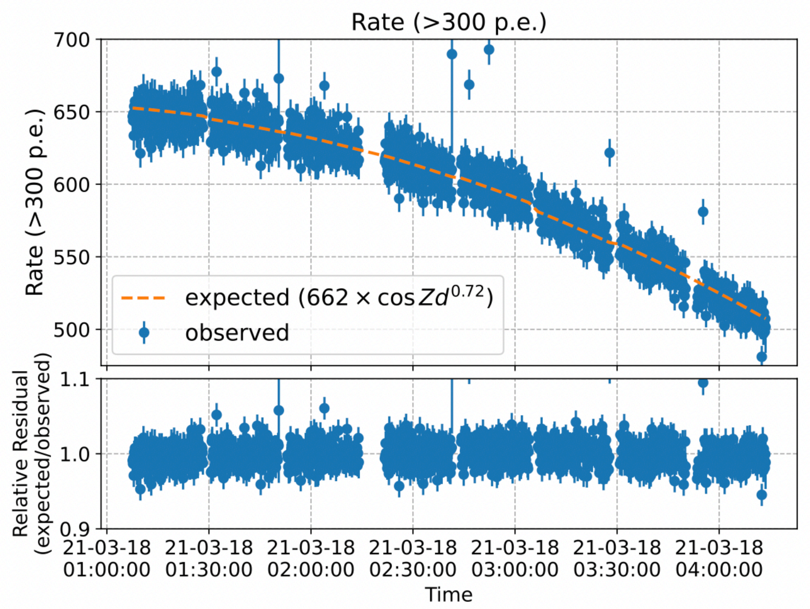

Figure 10 Time evolution of the rates above 300 p.e. cuts after the image cleaning (Top) and the relative residual (Bottom). The orange line shows the expected rates using the zenith.

ACKNOWLEDGEMENTS We gratefully acknowledge financial support from the agencies and organizations listed here: www.cta-observatory.org/consortium_acknowledgments

www.cta-observatory.org